

LBL-34409

Minijet-associated Dilepton Production in Ultrarelativistic Heavy Ion Collisions ^{*}

K. J. Eskola^{1,2} and Xin-Nian Wang¹

¹*Nuclear Science Division, Mailstop 70A-3307, Lawrence Berkeley Laboratory*

University of California, Berkeley, California 94720.

²*Laboratory of High Energy Physics, P.O. Box 9, SF-00014 University of Helsinki, Finland.*[†]

(Oct. 15, 1993)

Abstract

Dilepton production associated with minijets is calculated in ultrarelativistic heavy ion collisions using the first order approximation of the dilepton fragmentation functions of quarks and gluons. The full QCD evolution of the fragmentation functions is also studied. We find that the dilepton pairs from the fragmentation of minijets are comparable to direct Drell-Yan at $\sqrt{s} = 200$ AGeV for small dilepton invariant mass $M \sim 1\text{-}2$ GeV/c² while dominant over a large range of mass at $\sqrt{s} = 6400$ AGeV.

25.75.+r, 12.38.Bx, 13.87.Ce, 24.85.+p

Typeset using REVTEX

^{*}This work was supported by the Director, Office of Energy Research, Division of Nuclear Physics of the Office of High Energy and Nuclear Physics of the U.S. Department of Energy under Contract No. DE-AC03-76SF00098.

I. INTRODUCTION

In the search for a quark gluon plasma (QGP) in ultrarelativistic heavy ion collisions, electromagnetic signals are considered good probes of the dense matter [1]. Because of the large electromagnetic mean free path, leptons and photons produced by interacting (anti)quarks inside QGP can easily escape the hot and dense matter and carry the information of the system to the detector. Recent developments in parton transport phenomenology indicate that dileptons and photons could also reveal the dynamics of the early evolution of the a dense parton system [2–4]. However, like for all the proposed QGP signals, background must be understood and subtracted in order to distinguish the true features of a QGP. In general, there are two kinds of background sources for the thermal electromagnetic signals. One comes from the evolution of the hadronic phase and the decays of the produced hadrons. The other one is due to the initial parton scatterings at the very earliest stage of the heavy ion collisions. For dilepton production, the latter one is usually referred to as Drell-Yan (DY) processes [5].

In the lowest order, $\mathcal{O}(\alpha^2)$, the DY processes are simply quark-antiquark annihilations. First order contributions $\mathcal{O}(\alpha^2\alpha_s)$ in perturbative QCD (pQCD), originating from initial state radiation and virtual corrections, give rise to about the same amount of dilepton production as in the lowest order, which is often characterized by a so-called “*K*-factor” of about 2 [6,7]. These corrections are also responsible for large p_T tails of the dilepton transverse momentum spectrum. At small p_T , summation over the initial state soft gluon radiations generates a Sudakov form factor regularizing the perturbative low p_T production [8]. By now, there also exist matrix element calculations of the second order pQCD contributions, $\mathcal{O}(\alpha^2\alpha_s^2)$, to the *K*-factor [9].

In this paper, we will investigate dilepton production associated with minijet final state radiation in heavy ion collisions at collider energies. It is expected that at energies $\sqrt{s} \gtrsim 200$ AGeV, minijets [(anti)quarks and gluons with $p_T \sim$ few GeV/c] are produced abundantly via multiple semihard scatterings. These minijets have important contributions to particle

production, transverse energy and overall evolution of the formed quark-gluon system [10]–[13]. Therefore, it would be interesting to study dilepton bremsstrahlung from the initially produced minijets. Especially, it is important to know whether the dileptons associated with minijets could compete with the lower order DY processes at midrapidity and small invariant dilepton masses $M \sim 1 - 3 \text{ GeV}/c^2$, where a window for observing the thermal dileptons is expected [1].

Rather than strictly applying the almost complete $\mathcal{O}(\alpha^2 \alpha_s^2)$ results from the matrix element calculations [9], we take a different and simpler approach by calculating the dilepton fragmentation functions of the final state minijets. Unlike in the real photon fragmentation functions [14,15], the relatively large invariant masses $M \gg \Lambda$ of the dileptons fix the lower limit of the momentum scale of the QCD radiation processes. This makes the problem calculable in pQCD. In the leading logarithm approximation and in an axial gauge [16], the dilepton fragmentation functions can be calculated up to all orders in pQCD. Using the obtained fragmentation functions to convolute with minijet cross sections, we then compute the contribution to the dilepton production from the final state radiation of minijets. We will show how the associated production of $M \sim 1 - 2 \text{ GeV}/c^2$ dileptons from minijets with $p_T \geq 2 \text{ GeV}/c$ is comparable to the first order DY results at BNL Relativistic Heavy Ion Collider (RHIC) energies but becomes dominant at CERN Large Hadron Collider (LHC) energies, even up to masses $M \sim 5 - 10 \text{ GeV}/c^2$. We will also study the effects of nuclear modifications of the parton distributions, especially nuclear shadowing, to the dilepton rates.

The remainder of the paper is organized as follows. In the next Section, we will calculate the dilepton fragmentation functions in the framework of pQCD. The connection and the difference between real photon fragmentation functions are discussed. We will derive both the first order result and the one with QCD evolution, including corrections to all orders in pQCD. In Sec. III, the dilepton fragmentation functions are convoluted with hard and semihard parton scattering cross sections to calculate the minijet-associated dilepton production in heavy ion collisions at both RHIC and LHC energies. Finally, a summary with some discussions on the implications to the dilepton production from a QGP is given in Sec.

II. DILEPTON FRAGMENTATION FUNCTIONS

In this Section, we review the dilepton fragmentation functions of quark and gluon jets. We will work in an axial gauge so that interference terms in the final state radiation disappear in the leading logarithm approximation [16].

A. Lowest order in pQCD

Let us define z as the fractional light-cone momentum and q^2 as the virtuality of an off-shell parton as illustrated in Fig. 1(a). The differential cross section for a quark q_i produced in a hard process with momentum scale Q to emit a dilepton with invariant mass M is,

$$\frac{1}{\sigma_0} \frac{d\sigma}{dz dz_\ell dq^2 dM^2} = e_i^2 \frac{\alpha}{2\pi q^2} P_{q \rightarrow \gamma q}(z) \frac{\alpha}{2\pi M^2} P_{\gamma \rightarrow \ell^+ \ell^-}(z_\ell), \quad (1)$$

where e_i is the fractional charge of the quark q_i , σ_0 is the total cross section of the hard process, and

$$P_{q \rightarrow \gamma q}(z) = \frac{1}{z} [1 + (1 - z)^2], \quad (2)$$

$$P_{\gamma \rightarrow \ell^+ \ell^-}(z) = z^2 + (1 - z)^2, \quad (3)$$

are the splitting functions for $q \rightarrow \gamma q$ and $\gamma \rightarrow \ell^+ \ell^-$ which are similar to those of $q \rightarrow gq$ and $g \rightarrow q\bar{q}$, respectively, except for the color factors. Integrating over the virtuality q^2 of the intermediate quark and the fractional momentum z_ℓ of one of the leptons, one has the QED dilepton fragmentation function of a quark,

$$\begin{aligned} D_{\text{DL}/q_i}^{(0)}(z, M^2, Q^2) &\equiv \int_{M^2}^{Q^2} dq^2 \int_0^1 dz_\ell \frac{1}{\sigma_0} \frac{d\sigma}{dz dz_\ell dq^2 dM^2} \\ &= e_i^2 \left(\frac{\alpha}{2\pi} \right)^2 \frac{2}{3M^2} \ln \left(\frac{Q^2}{M^2} \right) \frac{1}{z} [1 + (1 - z)^2]. \end{aligned} \quad (4)$$

One can see that $D_{\text{DL}/q_i}^{(0)}(z, M^2, Q^2)$ is similar to a virtual photon fragmentation function, except for a factor due to the extra QED coupling and the integration over the relative phase space of the leptons,

$$D_{\text{DL}/q_i}^{(0)}(z, M^2, Q^2) = \frac{\alpha}{2\pi} \frac{2}{3M^2} D_{\gamma^*/q_i}^{(0)}(z, M^2, Q^2). \quad (5)$$

For a real photon fragmentation function, the lower limit for the integration over q^2 in Eq. 4 is in principle given by the quark mass. For massless quarks, the infrared divergence in the lowest order has to be regulated by some cutoff of the hadronic scale. In the absence of a large mass scale, the QCD corrections to real photon fragmentation function have also to be regulated by some cutoff. The physics below the cutoff becomes nonperturbative. One has to introduce some initial conditions for the real photon fragmentation functions, either given by experimental data or by some model-dependent assumptions. The problem of dilepton production is different because the fixed invariant mass M provides a natural cutoff below which kinematic restrictions will terminate the processes. The QCD processes above this cutoff are in principle calculable to all orders.

Since gluons are not directly coupled to photons and leptons, the dilepton fragmentation function of a gluon in the lowest order is,

$$D_{\text{DL}/g}^{(0)}(z, M^2, Q^2) = 0. \quad (6)$$

For later convenience, we define

$$\kappa(M, Q) \equiv \ln \left[\frac{\ln(Q^2/\Lambda^2)}{\ln(M^2/\Lambda^2)} \right], \quad (7)$$

and

$$Q_i^{(0)}(z) \equiv e_i^2 \frac{1}{z} [1 + (1 - z)^2], \quad (8)$$

so that we can rewrite Eq. 4 as

$$D_{\text{DL}/q_i}^{(0)}(z, M^2, Q^2) = \left(\frac{\alpha}{2\pi} \right)^2 \frac{2}{3M^2} \ln\left(\frac{M^2}{\Lambda^2}\right) (e^\kappa - 1) Q_i^{(0)}(z). \quad (9)$$

B. First order contributions

The first order contribution in pQCD to the dilepton fragmentation function of a quark comes from a gluon bremsstrahlung before the virtual photon production as shown in

Fig. 1(b). Remember now that $z = z_1 z_2$ is the fraction of the momentum, carried by the dilepton, of the initial quark before the gluon radiation. Defining the convolution of two functions as

$$A \otimes B(z) \equiv \int_z^1 \frac{dz_1}{z_1} A(z_1) B(z/z_1), \quad (10)$$

it is straightforward to write down the first order dilepton fragmentation function,

$$\begin{aligned} D_{\text{DL}/q_i}^{(1)}(z, M^2, Q^2) &= \int_{M^2}^{Q^2} dq_1^2 \frac{\alpha_s(q_1^2)}{2\pi q_1^2} \int_z^1 \frac{dz_1}{z_1} P_{q \rightarrow qg}(z_1) D_{\text{DL}/q_i}^{(0)}\left(\frac{z}{z_1}, M^2, Q^2\right) \\ &= \left(\frac{\alpha}{2\pi}\right)^2 \frac{2}{3M^2} \ln\left(\frac{M^2}{\Lambda^2}\right) \frac{2}{\beta_0} (e^\kappa - 1 - \kappa) P_{q \rightarrow qg} \otimes Q_i^{(0)}(z), \end{aligned} \quad (11)$$

where,

$$\alpha_s(q^2) = \frac{4\pi}{\beta_0 \ln(q^2/\Lambda^2)}, \quad \beta_0 = 11 - 2n_f/3, \quad (12)$$

is the running strong coupling constant with n_f quark flavors. The splitting function for $q \rightarrow qg$ in QCD is

$$P_{q \rightarrow qg}(z) = \frac{4}{3} \left[\frac{1+z^2}{1-z} \right]_+. \quad (13)$$

The “+” function here is introduced to include the virtual corrections to cancel the singularity from the soft gluon emission and to guarantee momentum conservation [16,17]. Other splitting functions we will use in the following are the standard ones [17],

$$P_{q \rightarrow gq}(z) = P_{q \rightarrow qg}(1-z), \quad (14)$$

$$P_{g \rightarrow q\bar{q}}(z) = \frac{1}{2} [z^2 + (1-z)^2], \quad (15)$$

$$P_{g \rightarrow gg}(z) = 6 \left[\frac{z}{(1-z)_+} + \frac{1-z}{z} + z(1-z) + \left(\frac{11}{12} - \frac{2n_f}{36}\right) \delta(1-z) \right]. \quad (16)$$

The convolution in Eq. 11 can be easily done and it gives,

$$\begin{aligned} Q_i^{(1)}(z) &\equiv P_{q \rightarrow qg} \otimes Q_i^{(0)}(z) \\ &= \frac{4e_i^2}{3z} \left\{ 2[1 + (1-z)^2] \ln(1-z) + (2-z)z \ln z + z(2 - \frac{1}{2}z) \right\}. \end{aligned} \quad (17)$$

To the first order in pQCD, the dilepton fragmentation function of a gluon is not zero anymore. From the diagram in Fig. 1(c), we have

$$\begin{aligned} D_{\text{DL}/g}^{(1)}(z, M^2, Q^2) &= \sum_{i=1}^{2n_f} \int_{M^2}^{Q^2} dq_1^2 \frac{\alpha_s(q_1^2)}{2\pi q_1^2} \int_z^1 \frac{dz_1}{z_1} P_{g \rightarrow q\bar{q}}(z_1) D_{\text{DL}/q_i}^{(0)}\left(\frac{z}{z_1}, M^2, Q^2\right) \\ &= \left(\frac{\alpha}{2\pi}\right)^2 \frac{2}{3M^2} \ln\left(\frac{M^2}{\Lambda^2}\right) \frac{2}{\beta_0} (e^\kappa - 1 - \kappa) \sum_{i=1}^{2n_f} P_{g \rightarrow q\bar{q}} \otimes Q_i^{(0)}(z), \end{aligned} \quad (18)$$

and the convolution in z can also be calculated explicitly in this case, giving

$$\begin{aligned} G^{(1)}(z) &\equiv \sum_{i=1}^{2n_f} P_{g \rightarrow q\bar{q}} \otimes Q_i^{(0)}(z) \\ &= \sum_{i=1}^{2n_f} e_i^2 \frac{1}{2z} \left[\frac{4}{3}(1 - z^3) + z(1 - z) + 2(1 + z)z \ln z \right]. \end{aligned} \quad (19)$$

As we will see below numerically, radiative corrections to any order will soften the QED fragmentation function of quarks and increase the fragmentation function of gluons. Because of the leading logarithm behavior of the radiations, the dependence of QCD corrections on the strong coupling constant is cancelled out so that they might become important to all orders. From Eqs. 9 and 11, we can see that the relative importance of the first order QCD correction to the QED fragmentation function is controlled by a Q -dependent factor,

$$C \sim 1 - \frac{\kappa}{e^\kappa - 1}, \quad (20)$$

where κ is defined in Eq. 7. For values of Q^2 not too large relative to M^2 , κ is very small so that higher order corrections can be neglected. Only for extremely large values of Q^2 and thus κ , C becomes comparable to 1. Then one has to include corrections to all orders. For our consideration here, Q^2 is in the order of p_T^2 of the minijets. Thus, as we will show in the next Section, for most of the minijet production with $p_T \sim 2$ GeV/c, first order calculation of the dilepton fragmentation functions should be sufficient.

C. Full QCD evolution

Following the same steps as we have calculated the first order corrections to the dilepton fragmentation functions, we can calculate the higher order contributions. Here we neglect

the further splitting of the radiated soft gluons and quarks, and only consider those diagrams with a simple ladder structure in leading logarithm approximation. Therefore, the radiated soft gluons and quarks are always on mass-shell. The general form of the contributions with n radiations before the dilepton production can be derived as

$$D_{\text{DL}/q_i}^{(n)}(z, M^2, Q^2) = \left(\frac{\alpha}{2\pi}\right)^2 \frac{2}{3M^2} \ln\left(\frac{M^2}{\Lambda^2}\right) \times \left(\frac{2}{\beta_0}\right)^n \left[e^\kappa - (1 + \kappa + \dots + \frac{\kappa^n}{n!})\right] Q_i^{(n)}(z), \quad (21)$$

$$D_{\text{DL}/g}^{(n)}(z, M^2, Q^2) = \left(\frac{\alpha}{2\pi}\right)^2 \frac{2}{3M^2} \ln\left(\frac{M^2}{\Lambda^2}\right) \times \left(\frac{2}{\beta_0}\right)^n \left[e^\kappa - (1 + \kappa + \dots + \frac{\kappa^n}{n!})\right] G^{(n)}(z), \quad (22)$$

where $Q_i^{(n)}(z)$ and $G^{(n)}(z)$ can be calculated iteratively from the lower order results via

$$Q_i^{(n)}(z) = P_{q \rightarrow qg} \otimes Q_i^{(n-1)}(z) + P_{q \rightarrow gg} \otimes G^{(n-1)}(z), \quad (23)$$

$$G^{(n)}(z) = \sum_{i=1}^{2n_f} P_{g \rightarrow q\bar{q}} \otimes Q_i^{(n-1)}(z) + P_{g \rightarrow gg} \otimes G^{(n-1)}(z). \quad (24)$$

Since we know $Q_i^{(0)}(z)$ (see Eq. 8) and $G^{(0)}(z) = 0$, we can in principle perform the above convolutions up to any order as we did for $Q_i^{(1)}(z)$ (Eq. 17) and $G^{(1)}(z)$ (Eq. 19), and obtain the full QCD dilepton fragmentation functions as,

$$D_{\text{DL}/q_i}(z, M^2, Q^2) = \sum_{n=0}^{\infty} D_{\text{DL}/q_i}^{(n)}(z, M^2, Q^2), \quad (25)$$

$$D_{\text{DL}/g}(z, M^2, Q^2) = \sum_{n=1}^{\infty} D_{\text{DL}/g}^{(n)}(z, M^2, Q^2). \quad (26)$$

For large values of n , evaluating the integration in the convolution analytically is obviously too cumbersome. One method to evaluate the full fragmentation functions is to solve numerically a set of coupled evolution equations.

Taking derivatives of $D_{\text{DL}/q_i,g}(z, M^2, Q^2)$ with respect to Q^2 and using

$$Q^2 \frac{d\kappa}{dQ^2} = \frac{1}{\ln(Q^2/\Lambda^2)}, \quad (27)$$

and the definition of $\alpha_s(Q^2)$ in Eq. 12, we can derive from Eqs. 21-26 the following coupled evolution equations,

$$\begin{aligned} \frac{dD_{\text{DL}/q_i}}{d \ln Q^2}(z, M^2, Q^2) &= \left(\frac{\alpha}{2\pi}\right)^2 \frac{2}{3M^2} Q_i^{(0)}(z) + \frac{\alpha_s(Q^2)}{2\pi} P_{q \rightarrow qg} \otimes D_{\text{DL}/q_i}(z, M^2, Q^2) \\ &\quad + \frac{\alpha_s(Q^2)}{2\pi} P_{q \rightarrow gq} \otimes D_{\text{DL}/g}(z, M^2, Q^2), \end{aligned} \quad (28)$$

$$\begin{aligned} \frac{dD_{\text{DL}/g}}{d \ln Q^2}(z, M^2, Q^2) &= \frac{\alpha_s(Q^2)}{2\pi} \sum_{i=1}^{2n_f} P_{g \rightarrow q\bar{q}} \otimes D_{\text{DL}/q_i}(z, M^2, Q^2) \\ &\quad + \frac{\alpha_s(Q^2)}{2\pi} P_{g \rightarrow gg} \otimes D_{\text{DL}/g}(z, M^2, Q^2). \end{aligned} \quad (29)$$

These evolution equations are very similar to those of real photon fragmentation functions [14,15] and the parton distribution functions in a photon [18]. The only difference is that dilepton (or virtual photon) fragmentation functions with a given mass M have a definite initial condition,

$$D_{\text{DL}/q_i,g}(z, M^2, Q^2) \Big|_{Q^2=M^2} = 0, \quad (30)$$

together with the boundary condition,

$$D_{\text{DL}/q_i,g}(z, M^2, Q^2) \Big|_{z=1} = 0. \quad (31)$$

The boundary condition simply means that the probability for the dilepton to take the whole fraction of momentum of the initial quark or gluon is zero after QCD evolution is taken into account. Since there is always a finite contribution to $dD_{\text{DL}/q_i}/dQ^2$ from the QED term in the evolution equation Eq. 28, one can verify that $D_{\text{DL}/q_i}(z, M^2, Q^2)$ must approach zero as $1/\ln(1-z)$ at $z = 1$ in order to satisfy the boundary condition at all Q^2 . For gluons, $D_{\text{DL}/g}(z, M^2, Q^2)$ must go to zero faster than $1/\ln(1-z)$.

The above evolution equations with the initial and boundary conditions can be solved numerically. The scale M^2 now sets the starting point of the evolution. We show the QCD-evolved dilepton fragmentation functions $zD_{\text{DL}/q_i,g}(z, M^2, Q^2)$ scaled by a common factor $(\alpha/2\pi)^2(2/3M^2)\ln(Q^2/M^2)$ in Fig. 2 for $M = 1 \text{ GeV}/c^2$ and $Q = 5 \text{ GeV}$. Together, we also show the analytical results to the lowest and first order. It is clear that both the first order corrections and the full QCD evolution soften the fragmentation functions. The overall QCD corrections to the QED (or lowest order in pQCD) result are about 10%, except near $z = 0$

and 1. Since a gluon does not have dilepton production to the zeroth order in pQCD, the dilepton fragmentation function of a gluon is one order of magnitude smaller than a quark. Because there are logarithmic divergences at $z = 0$ and 1 for each order correction to the dilepton fragmentation functions, as can be seen in Eqs. 17 and 19, every order becomes important so that one has to sum them together to get the full QCD result. This is why the full QCD-evolved fragmentation functions in Fig. 2 differ considerably from the first order results near $z = 0$ and 1. To the first order, the fragmentation function of a quark is exactly proportional to the square of its fractional charge, e_i^2 . This charge scaling is only slightly violated at small z for large Q due to the gluonic contribution to the QCD evolution as seen in Eq. 28.

III. ASSOCIATED DILEPTON PRODUCTION

A. Kinematical limits

In this paper, we are interested in the dilepton production cross section integrated over the transverse momentum. Hence, we need only the dilepton fragmentation functions integrated over z . As we have seen in the previous Section, the fragmentation functions diverge at $z = 0$. One must therefore introduce an infrared cutoff. Fortunately, for dilepton production, the invariant mass M provides a natural cutoff.

Assuming that Q^2 and q^2 are the virtualities of the parton before and after the emission of a virtual photon with fractional momentum z , one can verify that the relative transverse momentum of the dilepton with respect to the original parton is

$$k_T^2 = z(1-z) \left[Q^2 - \frac{M^2}{z} - \frac{q^2}{1-z} \right]. \quad (32)$$

Neglecting q^2 and requiring $k_T^2 \geq 0$, we can see that M^2 provides a natural kinematical cutoff for z ,

$$z \geq z_0 \equiv M^2/Q^2. \quad (33)$$

In principle, one could take into account these kinematical limits at every step of the radiation processes, as done in Monte Carlo approaches [19–22]. Although not shown here, this can be done analytically for the first order calculation of the dilepton fragmentation functions. One could also use the relative transverse momentum k_T^2 as the argument in the running strong coupling constant. This is, however, beyond the scope of our simple leading logarithm estimates in this paper.

With the kinematical cutoff in Eq. 33, we can obtain the integrated dilepton fragmentation functions, $D_{\text{DL}/q_i,g}(M^2, Q^2)$, the probabilities for a quark or gluon to produce a dilepton with mass M within the interval dM^2 . The lowest and first order fragmentation functions can be obtained analytically by integrating Eqs. 9, 11 and 18 over z ,

$$D_{\text{DL}/q_i}^{(0)}(M^2, Q^2) = e_i^2 \left(\frac{\alpha}{2\pi} \right)^2 \frac{2}{3M^2} \ln\left(\frac{M^2}{\Lambda^2}\right) (e^\kappa - 1) \\ \left\{ 2 \ln\left(\frac{Q^2}{M^2}\right) - \frac{3}{2} + 2 \frac{M^2}{Q^2} - \frac{1}{2} \frac{M^4}{Q^4} \right\}, \quad (34)$$

$$D_{\text{DL}/q_i}^{(1)}(M^2, Q^2) = e_i^2 \left(\frac{\alpha}{2\pi} \right)^2 \frac{2}{3M^2} \ln\left(\frac{M^2}{\Lambda^2}\right) \frac{2}{\beta_0} (e^\kappa - 1 - \kappa) \frac{4}{3} \\ \left\{ 4g_2\left(\frac{M^2}{Q^2}\right) - \frac{2\pi^2}{3} - \left(3 - \frac{M^2}{Q^2}\right) \left(1 - \frac{M^2}{Q^2}\right) \ln\left(1 - \frac{M^2}{Q^2}\right) \right. \\ \left. - \frac{M^2}{Q^2} \left(2 - \frac{1}{2} \frac{M^2}{Q^2}\right) \ln\left(\frac{M^2}{Q^2}\right) + \left(1 - \frac{M^2}{Q^2}\right) \left(\frac{5}{2} - \frac{1}{2} \frac{M^2}{Q^2}\right) \right\}, \quad (35)$$

$$D_{\text{DL}/g}^{(1)}(M^2, Q^2) = \left(\frac{\alpha}{2\pi} \right)^2 \frac{2}{3M^2} \ln\left(\frac{M^2}{\Lambda^2}\right) \frac{2}{\beta_0} (e^\kappa - 1 - \kappa) \frac{1}{2} \sum_i^{2n_f} e_{q_i}^2 \\ \left\{ \left(\frac{4}{3} + 2 \frac{M^2}{Q^2} + \frac{M^4}{Q^4}\right) \ln\left(\frac{Q^2}{M^2}\right) \right. \\ \left. - \frac{1}{9} \left(1 - \frac{M^2}{Q^2}\right) \left(22 + 13 \frac{M^2}{Q^2} + 4 \frac{M^4}{Q^4}\right) \right\}, \quad (36)$$

where the function $g_2(x)$ is defined as

$$g_2(x) = \sum_{n=1}^{\infty} \frac{x^n}{n^2}. \quad (37)$$

We plot in Fig. 3 the full QCD-evolved results $D_{\text{DL}/q_i,g}(M^2, Q^2)$ as functions of M^2 at fixed $Q=4$ GeV. The first order results $D_{\text{DL}/q_i}^{(0)}(M^2, Q^2) + D_{\text{DL}/q_i}^{(1)}(M^2, Q^2)$ and $D_{\text{DL}/g}^{(1)}(M^2, Q^2)$

are very close to the full QCD-evolved fragmentation functions with only a few percent difference through the whole M^2 range. As we have seen in Fig. 2, the full QCD-evolved fragmentation functions are enhanced at small z while depleted at large z as compared to the lowest order calculations. For small values of M^2/Q^2 , QCD evolution is important, but the lower limit z_0 of the z -integration is also small. Thus, the integrated full QCD fragmentation functions are almost the same as the first order results. At large values of M^2/Q^2 , the lower limit z_0 is large, but the QCD corrections in any order are increasingly smaller. Therefore, in the whole range of M^2 , the first order calculation of the z -integrated dilepton fragmentation functions is a very good approximation.

B. Dilepton production associated with minijets

In the following, we consider dilepton production associated with minijets. In particular, we are interested in the differential rates of dileptons with rapidity $Y = 0$ as functions of the invariant mass M . As a first approximation, we can assume the dilepton to be produced collinearly with the parent quark or gluon. Then the differential cross section can be written down in a straightforward manner by folding the z -integrated dilepton fragmentation functions $D_{\text{DL}/q_i}(M^2, Q^2)$ and $D_{\text{DL}/g}(M^2, Q^2)$ with the $2 \rightarrow 2$ subprocesses of minijet production. We can also neglect the contribution from the initial state dilepton radiation, since the rapidities of these pairs are typically large like those of the initially radiated partons [23]. One has to take into account that the dilepton pair can be produced by either one of the final state partons, and connect this to the correct normalization of the integrated minijet cross section σ_{jet} . In this way, the basic formula for the associated production of dileptons with $Y \sim 0$ from minijets in a AA collision at impact parameter b can be written as follows:

$$\frac{dN_{AA}^{\text{DL/jet}}(b)}{dM^2 dY} = \frac{1}{2} \int d^2 r_\perp \int_{p_0^2}^{s/4} dp_T^2 dy_1 dy_2 \sum_{\substack{abcd= \\ q,\bar{q},g}} x_1 f_{a/A}(x_1, Q^2, r_\perp) x_2 f_{b/A}(x_2, Q^2, |\mathbf{b} - \mathbf{r}_\perp|) \frac{d\sigma^{ab \rightarrow cd}}{dt}(\hat{s}, \hat{t}, \hat{u}) \left\{ D_{\text{DL}/c}(M^2, Q_{\max}^2) \delta(Y - y_1) + D_{\text{DL}/d}(M^2, Q_{\max}^2) \delta(Y - y_2) \right\}, \quad (38)$$

where the produced (anti)quarks and gluons (i.e. minijets) have transverse momentum $p_0 \leq p_T \leq \sqrt{s}/2$ and the kinematical range of rapidities

$$|y_1| \leq \ln\left(\frac{\sqrt{s}}{2p_T} + \sqrt{\frac{s}{4p_T^2} - 1}\right) \quad (39)$$

$$-\ln\left(\frac{\sqrt{s}}{p_T} - e^{-y_1}\right) \leq y_2 \leq \ln\left(\frac{\sqrt{s}}{p_T} - e^{y_2}\right). \quad (40)$$

The momentum fractions of the initial state partons are denoted by

$$x_{1,2} = \frac{p_T}{\sqrt{s}} (e^{\pm y_1} + e^{\pm y_2}), \quad (41)$$

and the Mandelstam variables in the parton-parton level for the massless partons by

$$\hat{s} = x_1 x_2 s = 2p_T^2 (1 + \cosh(y_1 - y_2)), \quad (42)$$

$$\hat{t} = -p_T^2 (1 + e^{y_2 - y_1}), \quad (43)$$

$$\hat{u} = -p_T^2 (1 + e^{y_1 - y_2}). \quad (44)$$

The cross sections $d\sigma^{ab \rightarrow cd}/d\hat{t} \sim \mathcal{O}(\alpha_s^2)$ for the various partonic subprocesses can be found e.g. in Refs. [14,24]. The parton density of a nucleus by our definition is

$$f_{a/A}(x, Q^2, r_\perp) = t_A(r_\perp) R_{a/A}(x, Q^2, r_\perp) f_{a/N}(x, Q^2), \quad (45)$$

where $t_A(r_\perp)$ is the thickness function of the nucleus which is normalized to $\int d^2 r_\perp t_A(r_\perp) = A$. The parton distribution in a nucleon is $f_{a/N}(x, Q^2)$, and the ratio $R_{a/A}(x, Q^2, r_\perp)$ for the nuclear modifications to the parton distributions is both scale and impact parameter dependent [11,25]. In the following, we will approximate the impact parameter dependent ratio $R_{a/A}(x, Q^2, r_\perp)$ by its averaged value,

$$R_{a/A}(x, Q^2) \equiv \frac{1}{A} \int d^2 r_\perp t_A(r_\perp) R_{a/A}(x, Q^2, r_\perp), \quad (46)$$

so that

$$f_{a/A}(x, Q^2, r_\perp) \approx t_A(r_\perp) f_{a/\langle N \rangle}^A(x, Q^2), \quad (47)$$

where the effective parton distributions per nucleon in a nucleus is defined as

$$f_{a/\langle N \rangle}^A(x, Q^2) \equiv R_{a/A}(x, Q^2) f_{a/N}(x, Q^2). \quad (48)$$

In this paper we will use the set 1 of the Duke-Owens parton distributions [26] for $f_{a/N}(x, Q^2)$. We use the scale dependent nuclear modifications for $R_{a/A}(x, Q^2)$ as studied in [27]. Especially, we assume that at the lowest scale $Q = 2$ GeV, gluons are shadowed by the same amount as the structure function F_2^A in deeply inelastic ℓA scatterings. Note that the normalization of Eq. 38 can be checked by setting the M^2 -integrated fragmentation functions to unity and integrating over Y ; this will give us $2\sigma_{\text{jet}}(p_0, \sqrt{s})$ as expected when integrating over the inclusive $2 \rightarrow 2$ scattering cross section.

As usually in the case of pQCD calculations, there are uncertainties in choosing the momentum scales both in the parton distributions and the fragmentation functions. We will choose the scale entering the parton distributions to be the transverse momentum of the jets, $Q = p_T$, for Duke-Owens parametrization set 1 with $\Lambda = 0.2$ GeV [14]. The scale Q_{\max}^2 in the dilepton fragmentation functions represents the maximum virtuality of the final state parton before any radiation. As we have emphasized in this paper, the dilepton fragmentation functions at large fixed mass do not have nonperturbative contributions. Therefore, unlike the scale in the parton distributions, Q_{\max} in large mass dilepton fragmentation functions is not correlated with the choice of Λ . Examining the matrix elements of $a + b \rightarrow a + b + \gamma^*$ processes, one can find out that the scale entering the leading logarithm term is one of the Mandelstam variables, $\hat{s}, -\hat{t}, -\hat{u}$, depending on the channel of the specific process. However, in Eq. 38, we convolute the fragmentation functions with jet cross sections which include different channels and their interference terms. Therefore, Q_{\max} in Eq. 38 is only an effective momentum scale. From Eqs. 42-44, we know at least that $Q_{\max} \geq p_T$. We will discuss the sensitivity to the choice of Q_{\max} when we present the results of our calculation.

Note also that for the minijet production the lower limit p_0 of the integration over p_T is a parameter which determines the division between calculable “hard” and model-dependent “soft” processes. Most of the minijets are produced with $p_T \sim p_0 \sim$ few GeV/c, and they are basically nonresolvable as distinct E_T -clusters, even in hadronic collisions [28]. The

phenomenological value of p_0 depends on the model for σ_{soft} of soft processes, the parton distribution functions and the corresponding scale choice. Since these issues can not be addressed within pQCD, the possible range of values of p_0 has to be determined phenomenologically, in connection with a model for the soft contribution σ_{soft} to the particle production in pp and $p\bar{p}$ collisions [11,12,29,30]. We will use here $p_0 = 2 \text{ GeV}/c$, as suggested and studied in detail in Ref. [31]. Although already exactly calculated for inclusive jet production [32], the $\mathcal{O}(\alpha_s^3)$ contributions to the lowest order parton cross sections are simulated here by an overall factor $K \sim 2$. Clearly, the parameter p_0 depends also on the size of the next-to-leading order terms. We want to point out, however, that the cross section for the associated dilepton production in Eq. 38 is much less sensitive to the choice of p_0 than the minijet cross section itself. For $Q_{\text{max}} = p_T$, the dilepton fragmentation functions vanish for $M \geq p_T$. Whenever $M > p_0$, M takes over as an effective cutoff in the integration over p_T in Eq. 38. Therefore, the cross section for the associated dilepton production does not depend on the exact choice of p_0 at large M .

The symmetrized formula of Eq. 38 can be somewhat simplified by considering all the possible pairs of partons in the initial and final states, $\langle ab \rangle, \langle cd \rangle$. By changing the integration variables $y_{1,2}$ into $-y_{2,1}$ appropriately in the other half of the expression, and by using the \hat{t}, \hat{u} -symmetries of the subprocess cross sections, a $Y \leftrightarrow -Y$ symmetric formula can be written down. Especially, at $Y = 0$ we get:

$$\begin{aligned} \frac{dN_{AA}^{\text{DL/jet}}(b)}{dM^2 dY} \Big|_{Y=0} &= 2T_{AA}(b) \int_{p_0^2}^{s/4} dp_T^2 dy_2 \sum_{\substack{\langle ab \rangle \\ \langle cd \rangle}} \frac{1}{1 + \delta_{ab}} \frac{1}{1 + \delta_{cd}} x_1 f_{a/\langle N \rangle}^A(x_1, Q^2) x_2 f_{b/\langle N \rangle}^A(x_2, Q^2) \\ &\quad \left\{ D_{\text{DL}/c}(M^2, Q_{\text{max}}^2) \frac{d\sigma^{ab \rightarrow cd}}{d\hat{t}}(\hat{s}, \hat{t}, \hat{u}) + D_{\text{DL}/d}(M^2, Q_{\text{max}}^2) \frac{d\sigma^{ab \rightarrow cd}}{d\hat{t}}(\hat{s}, \hat{u}, \hat{t}) \right\} \Big|_{y_1=0}, \end{aligned} \quad (49)$$

where $T_{AA}(b) = \int d^2 r_\perp t_A(r_\perp) t_A(|\mathbf{b} - \mathbf{r}_\perp|)$ is the nuclear overlap function of the two colliding nuclei.

As discussed in the previous Section, the first order results in Eqs. 34-36 are a good approximation for the full z -integrated dilepton fragmentation functions, which is the approximation we shall adopt in what follows. The results from Eq. 49 with nuclear modifications

to the parton distributions are shown in Fig. 4 (solid curves) for $\sqrt{s} = 200$ AGeV and 6400 AGeV, respectively. In the figure, we have compared the minijet associated production of dileptons to the lowest order differential cross section of the direct Drell-Yan process (dashed curves),

$$\begin{aligned} \frac{dN_{AA}^{\text{DY}}(b)}{dM^2 dY} \Big|_{Y=0} = T_{AA}(b) \frac{4\pi\alpha^2}{9M^4} \sum_i e_{q_i}^2 & \left[x_1 f_{q_i/\langle N \rangle}^A(x_1, M^2) x_2 f_{\bar{q}_i/\langle N \rangle}^A(x_2, M^2) \right. \\ & \left. + x_1 f_{\bar{q}_i/\langle N \rangle}^A(x_1, M^2) x_2 f_{q_i/\langle N \rangle}^A(x_2, M^2) \right], \end{aligned} \quad (50)$$

where $x_{1,2} = M/\sqrt{s}$ at $Y = 0$. We have chosen the scale in the parton distributions as $Q = M$. To simulate the first order pQCD contributions to the DY cross section [6,7], we multiply Eq. 50 by an overall factor $K_{\text{DY}} \sim 2$. Note that since we have used the Duke-Owens parton distributions, which extend only down to $Q_0 = 2$ GeV, the results for direct Drell-Yan cannot really be trusted much below $M = 2$ GeV/c².

To study the sensitivity of the minijet associated dilepton production to the choice of the scale Q_{max} in the fragmentation functions, we plot in Fig. 4 the results of Eq. 49 for both $Q_{\text{max}} = p_T$ and $2p_T$. It is apparent that the results are relatively sensitive to the choice of Q_{max} . As we can understand from Eqs. 34-36, the difference between the two solid curves is due to the fact that the z -integrated fragmentation functions are proportional to $\ln^2(Q_{\text{max}}^2/M^2)$. Due to the kinematical restriction $M \leq Q_{\text{max}}$, changing $Q_{\text{max}} = 2p_T$ to p_T also effectively doubles the lower limit of the integration over p_T for fixed M in Eq. 49. This is the reason why the two solid curves have different slopes. As one of the main purposes of this paper, Fig. 4 demonstrates how the relative contribution of the dileptons associated with minijets in the range $1 \lesssim M \lesssim 10$ GeV/c² changes with increasing energy as compared to the direct Drell-Yan production. Even after taking into account the uncertainties due to different choices of Q_{max} , it can be seen clearly that at RHIC energy, $\sqrt{s} = 200$ AGeV, dileptons from the bremsstrahlung of minijets are comparable to the direct Drell-Yan at $M \lesssim 2$ GeV/c². However, when going up to TeV energy range, dileptons associated with minijets become more important, and dominate the Drell-Yan at LHC energy, $\sqrt{s} = 6400$ AGeV, even up to masses $M \sim 10$ GeV/c². Qualitatively, our results are similar to the

minijet-associated photon production in Ref. [33] where real photon fragmentation functions in the lowest order are considered.

To demonstrate the effects of parton shadowing and antishadowing, we plot in Fig. 5 the results calculated with (solid) and without (dashed curves) nuclear modifications of the parton distribution functions. We can see that nuclear shadowing depletes the Drell-Yan dileptons relatively more than the dileptons from the minijets. The basic reason for this is that Drell-Yan pair production dN_{AA}^{DY} in Eq. 50 as a function of $M = x_{1,2}\sqrt{s}$ probes the (anti)quark distributions directly, at least in the lowest order. Furthermore, the antiquark shadowing does not vary strongly with the scale M , as has been experimentally measured [34,35]. On the other hand, in the minijet-associated dilepton production, we have to integrate the contribution over the whole range of x . In addition, we also have to integrate over the scale $Q = p_T$. The gluon shadowing [27] we used here has stronger Q dependence than the (anti)quark. Therefore, the net effect of the nuclear modifications of the parton distributions to the minijet-associated dilepton production remains relatively small even at TeV energy range.

IV. SUMMARY AND DISCUSSION

In this paper, we have studied minijet-associated dilepton production in ultra-relativistic nuclear collisions. We calculated both the first order approximation and the full pQCD evolution of the dilepton fragmentation functions of produced partons. The dilepton pairs from the fragmentation of minijets are found to be comparable to direct Drell-Yan at RHIC energy for small invariant mass $M \sim 1\text{--}2 \text{ GeV}/c^2$. At LHC energy, the associated dilepton production becomes dominant over a relative large range of the invariant mass. These dileptons plus the direct Drell-Yan pairs would constitute part of the background to the dilepton production from a QGP and its pre-equilibrium stage. Other background includes dileptons from final hadronic rescatterings [36,37] and the decay of charmed hadrons [33,38].

It is also straightforward to calculate the p_T distribution of the associated dilepton pairs in

our fragmentation function approach. Since one has to convolute the dilepton fragmentation functions in z together with the p_T distributions of the jets, we expect the resultant p_T spectrum of these dileptons to be softer than the p_T spectrum of the jets. Therefore, the dileptons associated with minijets should have smaller p_T relative to the direct Drell-Yan pairs which have a high p_T tail like that of the produced jets. Since thermally produced dileptons in a QGP also have relatively small p_T as compared to Drell-Yan [1], minijet-associated dileptons thus pose a more intangible background.

In calculating the dilepton fragmentation functions, we have assumed leading logarithm approximation so that we can include contributions from all orders in pQCD. However, the higher order corrections are small and the first order results are sufficient enough for our estimates of the minijet-associated dilepton production. The largest uncertainty in our calculation is the choice of the momentum scale Q_{\max} used in the dilepton fragmentation functions. Since the correct scale in a matrix element calculation is channel-dependent, we used only an effective scale choice in the fragmentation functions to convolute with the minijet cross sections. We evaluated the dilepton spectrum for two choices of the scale, $Q_{\max} = p_T, 2p_T$. However, the results with $Q_{\max} = p_T$ should give us the lower bound of the associated dilepton production. Another notorious uncertainty of the p_T cutoff p_0 in minijet-related problems is greatly reduced here due to the kinematic restriction $M \leq Q_{\max}$. For $Q_{\max} = p_T$, the p_T cutoff is replaced by M whenever M is larger than p_0 .

The abundance of dileptons associated with minijet production at high energies is mainly due to the large gluon-related minijet cross sections and the high initial gluon densities inside the colliding nuclei. This should have important implications for the dilepton production in the pre-equilibrium stage of the quark gluon plasma. As pointed out recently [39–41], the parton system is not at all in chemical equilibrium when initially produced in the earliest stage of high energy nucleus-nucleus collisions. Because of the small cross sections for (anti)quark production, the initial parton system is dominated by gluons and is quark deficient as compared to an equilibrated QGP. Studies [39–41] also suggest that the parton system thus produced may not be able to achieve chemical equilibrium before hadronization.

In this case, dilepton production through $q\bar{q}$ annihilation should be severely suppressed. On the contrary, dilepton production from gluon fragmentation could become relatively important for a gluon dominated system, since gluon-related cross sections of small angle scatterings are about 9/4 larger than the quark. Even though the dilepton fragmentation function of a gluon is about one order of magnitude smaller than a quark, a gluon density at least about 5 times higher than the quark could easily compensate the small fragmentation function and make the gluon associated dilepton production important.

ACKNOWLEDGMENTS

We thank S. Gupta and K. Kajantie for helpful discussions. KJE thanks Magnus Ehrnrooth foundation, Oskar Öflund foundation, and Suomen Kulttuurirahasto for partial financial support. This work was supported by the Director, Office of Energy Research, Division of Nuclear Physics of the Office of High Energy and Nuclear Physics of the U.S. Department of Energy under Contract No. DE-AC03-76SF00098.

REFERENCES

† Present address.

- [1] P. V. Ruuskanen, Nucl. Phys. A **544**, 169c (1992).
- [2] J. I. Kapusta, L. McLerran and D. K. Srivastava, Phys. Lett. B **283**, 145 (1992).
- [3] K. Geiger and J. I. Kapusta, Phys. Rev. Lett. **70**, 1920 (1993).
- [4] E. Shuryak and L. Xiong, Phys. Rev. Lett. **70**, 2241 (1993).
- [5] S. D. Drell and T.-M. Yan, Phys. Rev. Lett. **25**, 316 (1970).
- [6] G. Altarelli, R. K. Ellis and G. Martinelli, Nucl. Phys. B **157**, 461 (1979); J. Kubar, M. Le Bellac, J. L. Meunier and G. Plaut, Nucl. Phys. B **175**, 251 (1980).
- [7] F. Khalafi and W. J. Stirling, Z. Phys. C **18**, 315 (1983).
- [8] Yu. L. Dokshitzer, D. I. D'yakonov and S. I. Troyan, Phys. Lett. B **78**, 290 (1978); Phys. Rep. **58**, 269 (1980); G. Parisi and R. Petronzio, Nucl. Phys. B **154**, 427 (1979); G. Altarelli, R. K. Ellis, M. Greco and G. Martinelli, Nucl. Phys. B **246**, 12 (1984); G. Altarelli, R. K. Ellis, and G. Martinelli, Phys. Lett. B **151**, 457 (1985).
- [9] A. N. Schellekens and W. L. van Neerven, Phys. Rev. D **21**, 2619 (1980); *ibid.* **22**, 1623 (1980); T. Matsuura, S. C. van der Marck and W. L. van Neerven, Nucl. Phys. B **319**, 570 (1989); T. Matsuura, R. Hamberg and W. L. van Neerven, *ibid.* **345**, 331 (1990).
- [10] K. Kajantie, P. V. Landshoff and J. Lindfors, Phys. Rev. Lett. **59**, 2517 (1987); K. J. Eskola, K. Kajantie and J. Lindfors, Nucl. Phys. B **323**, 37 (1989).
- [11] X.-N. Wang and M. Gyulassy, Phys. Rev. D **44**, 3501 (1991); Phys. Rev. D **45**, 844 (1992).
- [12] K. Geiger and B. Müller, Nucl. Phys. B **369**, 600 (1992); K. Geiger, Phys. Rev. D **47**, 133 (1993).

- [13] I. Kawrakow, H.-J. Möhring, and J. Ranft, Nucl. Phys. A **544**, 471c (1992).
- [14] J. F. Owens, Rev. Mod. Phys. **59**, 465 (1987).
- [15] M. Glück, K. Grassie, and E. Reya, Phys. Rev. D **30**, 1447 (1984); *ibid.* **45**, 3986 (1992); *ibid.* **46**, 1973 (1992).
- [16] See e.g. R. D. Field, Applications of Perturbative QCD, *Frontiers in Physics*, Vol. 77 (Addison-Wesley, 1989).
- [17] G. Altarelli and G. Parisi, Nucl. Phys. B **126**, 298 (1977).
- [18] R. J. DeWitt, L. M. Jones, J. D. Sullivan, D. E. Williams, and H. D. Wyld, Jr., Phys. Rev. D **19**, 2046 (1979); **20**, 1751(E) (1979).
- [19] K. Kajantie and E. Pietarinen, Phys. Lett. B **93**, 269 (1980).
- [20] G. Marchesini and B. R. Webber, Nucl. Phys. B **238**, 1 (1984).
- [21] T. Sjöstrand, Comput. Phys. Commun. **39**, 347 (1986); T. Sjöstrand and M. Bengtsson, *ibid.* **43**, 367 (1987).
- [22] R. Odorico, Nucl. Phys. B **172**, 157 (1980).
- [23] K. J. Eskola and X.-N. Wang, LBL preprint LBL-34156, 1993.
- [24] I. Sarcevic, S. D. Ellis and P. Carruthers, Phys. Rev. D **40**, 1446 (1989).
- [25] K. J. Eskola, Z. Phys. C **51**, 633 (1991).
- [26] D. W. Duke and J. F. Owens, Phys. Rev. D **30**, 50 (1984).
- [27] K. J. Eskola, Nucl. Phys. B **400**, 240 (1993).
- [28] UA1 collaboration, C. Albajar *et al.*, Nucl. Phys. B **309**, 405 (1988).
- [29] T. Sjöstrand and M. van Zijl, Phys. Rev. D **36**, 2019 (1987).
- [30] X.-N. Wang, Phys. Rev. D **46**, R1900 (1992); D **47**, 2754 (1993).

- [31] X.-N. Wang, Phys. Rev. D **43**, 104 (1991).
- [32] S. D. Ellis, Z. Kunszt and D. E. Soper, Phys. Rev. Lett **64**, 2121 (1990); Z. Kunszt and D. E. Soper, Phys. Rev. D **46**, 192 (1992).
- [33] S. Gupta, Phys. Lett. B **248**, 453 (1990).
- [34] EM collaboration, M. Arneodo *et al.*, Nucl. Phys. B **333**, 1 (1990).
- [35] NM collaboration, P. Amaudruz *et al.*, Z. Phys. C **51**, 387 (1991).
- [36] L. Xiong, Z. G. Wu, C. M. Ko and J. Q. Wu, Nucl. Phys. A **512**, 772 (1990).
- [37] C. Gale and J. I. Kapusta, Phys. Rev. C **38**, 2659 (1988).
- [38] R. Vogt, B. V. Jacak, and P. V. Ruuskanen, Proceedings of Quark-Matter'93, Borlänge, Sweden, June 20-24, 1993.
- [39] T. B. Biró, E. van Doorn, B. Müller, T. H. Thoma, and X. N. Wang, Duke University preprint DUKE-TH-93-46, to appear in Phy. Rev. C.
- [40] K. Geiger and J. I. Kapusta, Phys. Rev. D **47**, 4905 (1993).
- [41] K. J. Eskola and M. Gyulassy, Phys. Rev. C **47**, 2329 (1993).

FIGURES

FIG. 1. Illustration of the diagrams of (a) the lowest order, (b) the first order contributions in pQCD to the dilepton fragmentation functions of quarks and (c) gluons. The dashed lines present the associated hard processes with momentum scale Q .

FIG. 2. The QCD-evolved (solid), the lowest order (dot-dashed) and the first order (dashed) approximations of dilepton fragmentation functions $zD_{\text{DL}/a}(z, M^2, Q^2)$ of a u -quark and a gluon, for $M = 1 \text{ GeV}/c^2$ and $Q = 5 \text{ GeV}$. A factor $(\alpha/2\pi)^2(2/3M^2) \ln(Q^2/M^2)$ is divided out.

FIG. 3. The z -integrated dilepton fragmentation functions $D_{\text{DL}/a}(M^2, Q^2)$ for a u -quark (solid) and a gluon (dashed) as functions of M^2 at fixed $Q = 4 \text{ GeV}$. A factor $(\alpha/2\pi)^2 2/3M^2$ is divided out. The curve for gluon fragmentation is multiplied by 10.

FIG. 4. Mass spectra of minijet-associated (solid curves) and Drell-Yan (dashed) dileptons at $Y = 0$ in central $Au + Au$ collisions at $\sqrt{s} = 200$ and 6400 AGeV . The two solid curves correspond to two choices of the scale $Q_{\text{max}} = p_T$ and $2p_T$ in the dilepton fragmentation functions. Parton shadowing is included in the calculations.

FIG. 5. Mass spectra of the minijet-associated and Drell-Yan dileptons in central $Au + Au$ collisions at $\sqrt{s} = 200$ and 6400 AGeV , with (solid) and without (dashed) parton shadowing. For the associated production, the scale in the dilepton fragmentation functions is chosen to be $Q_{\text{max}} = 2p_T$.

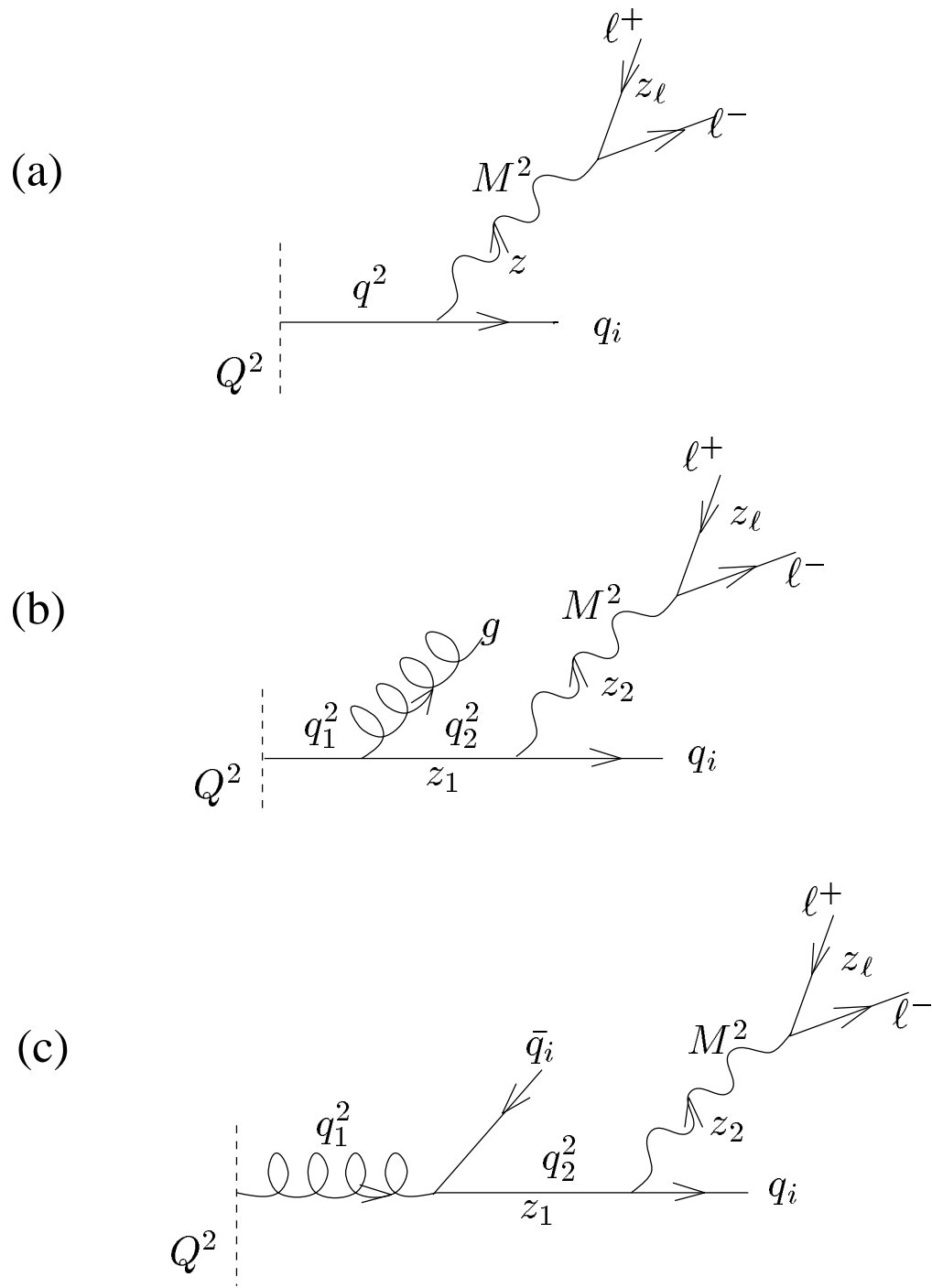


Fig. 1

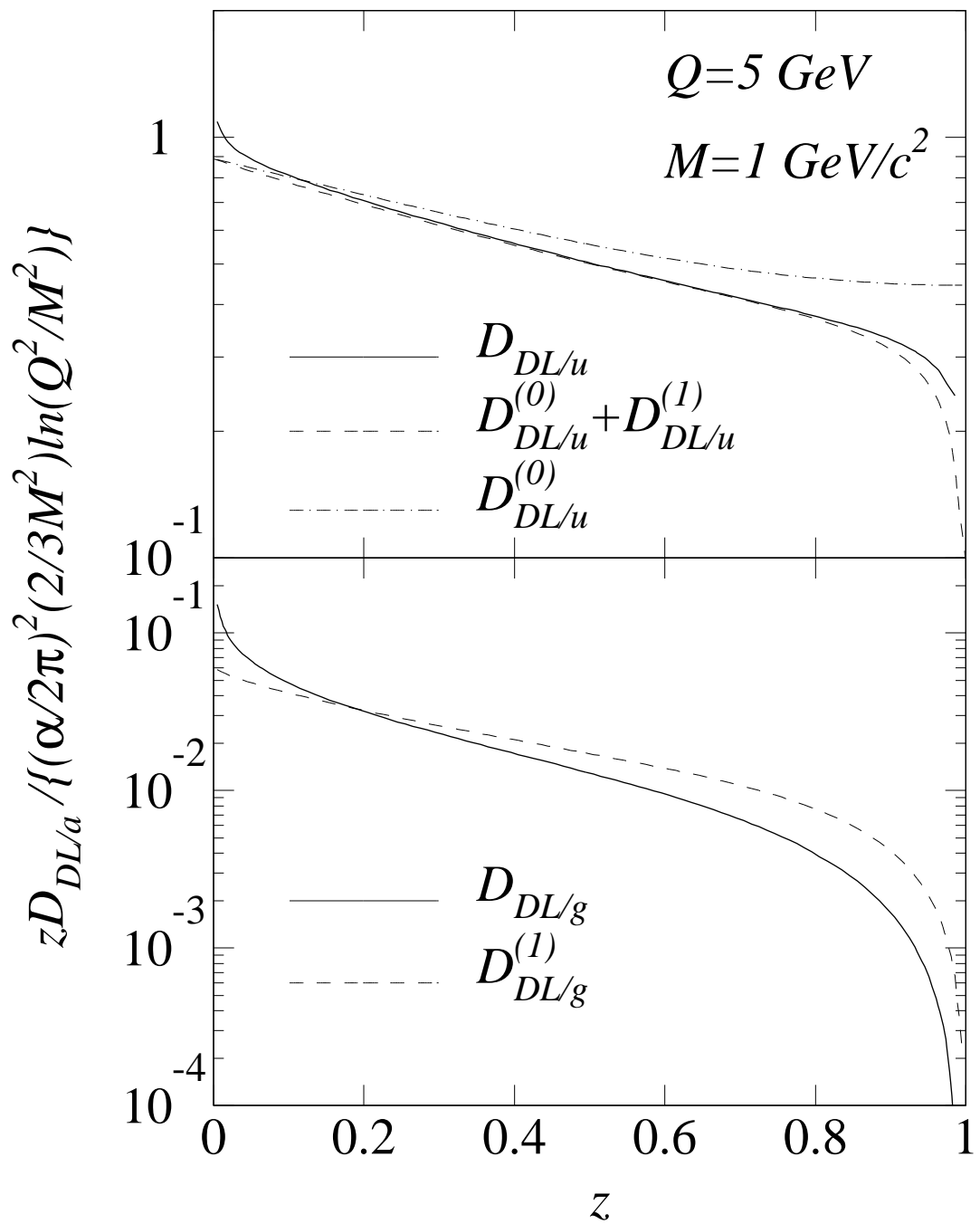


Fig. 2

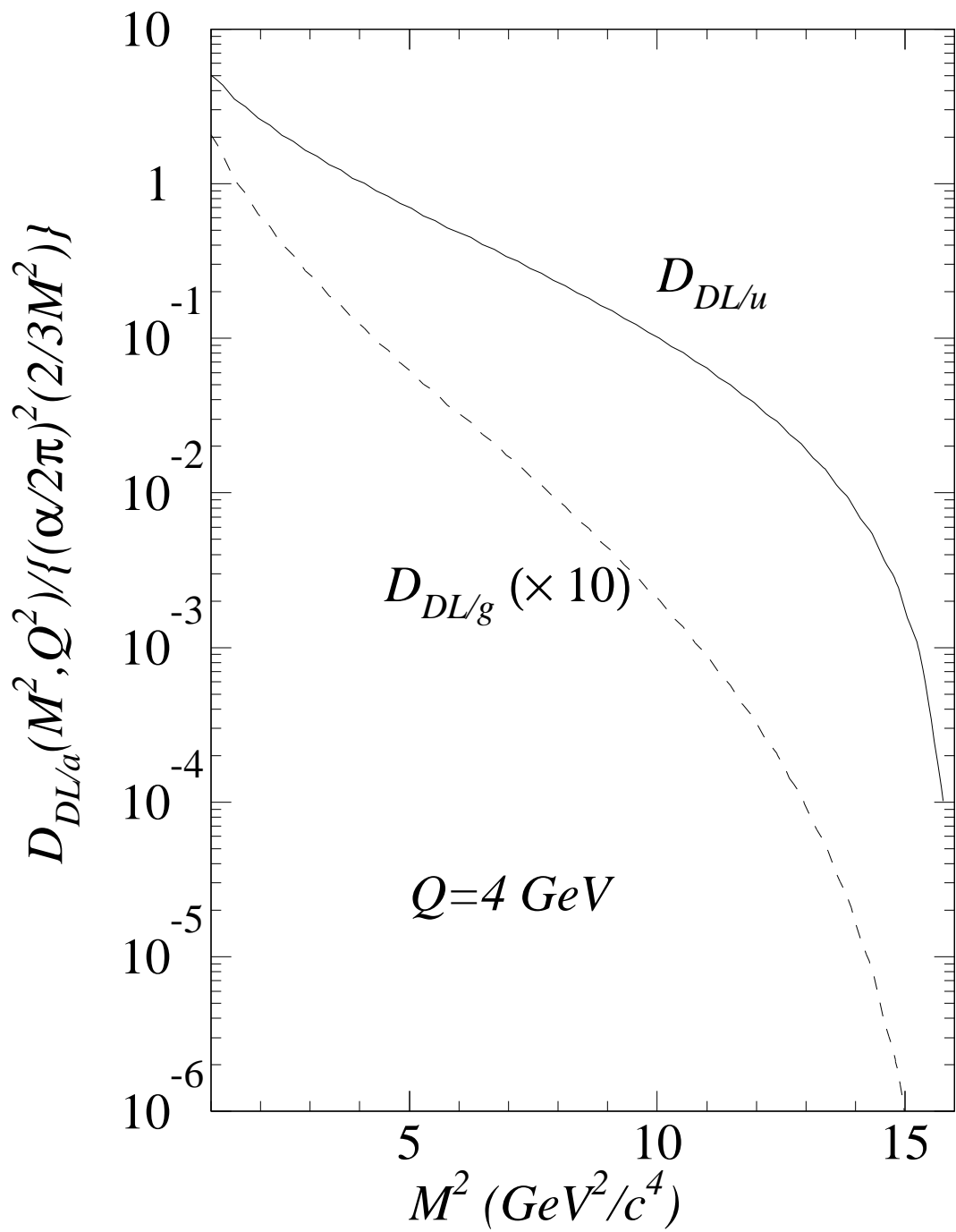


Fig. 3

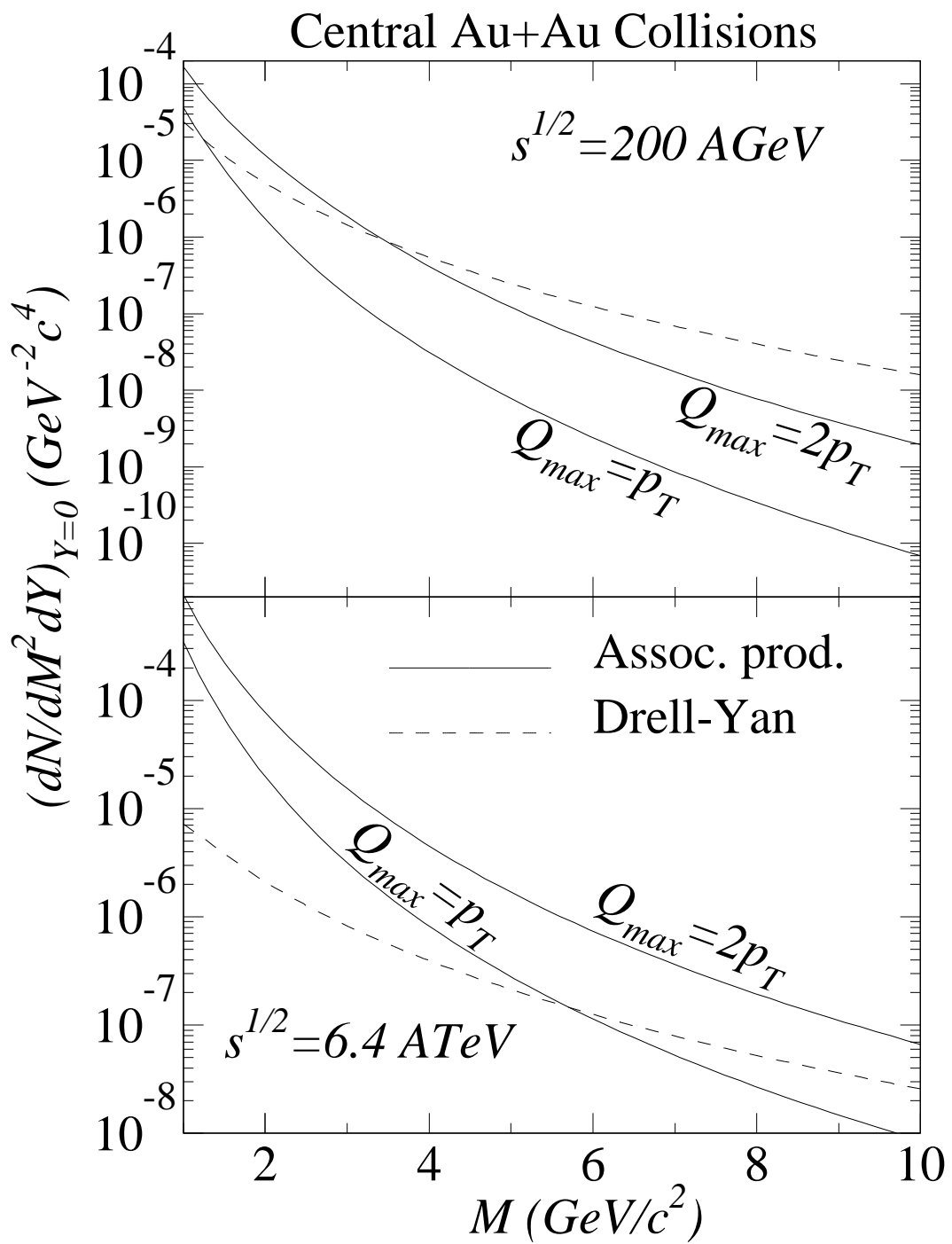


Fig. 4

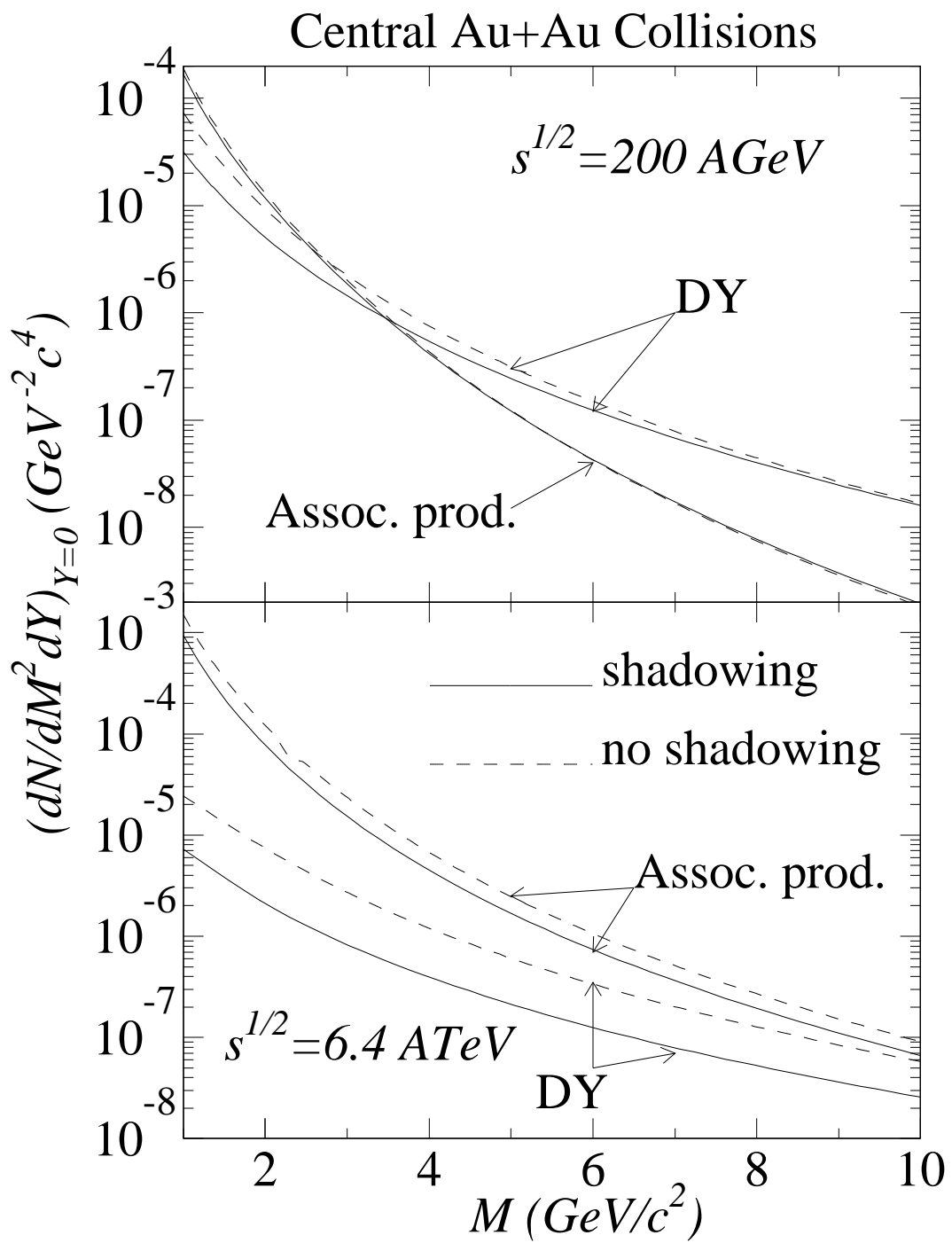


Fig. 5